Soft Matter

RSC Publishing

PAPER

View Article Online
View Journal | View Issue

Cite this: *Soft Matter*, 2013, **9**, 5716

Diffusion mechanisms in smectic ionic liquid crystals: insights from coarse-grained MD simulations†

Giacomo Saielli,*[a] Gregory A. Voth[b] and Yanting Wang[c]

Received 5th February 2013
Accepted 11th April 2013

DOI: 10.1039/c3sm50375e

www.rsc.org/softmatter

We present the results of MD simulations, using a coarse grained force field, concerning the mechanism of diffusion in ionic liquid crystals. The dynamical properties of the recently characterized (G. Saielli, *Soft Matter*, 2012, **8**, 10279) model system of 1-hexadecyl-3-methylimidazolium nitrate in the smectic A phase are analysed in detail. Comparison is made with the dynamical behaviour of thermotropic non-ionic smectic liquid crystals (LCs) and with that of lamellar phases of surfactant–water mixtures. The self-diffusion anisotropy, that is the ratio between the parallel and perpendicular diffusion coefficients, is consistent with that of non-ionic smectic LCs, though a significant contribution to the parallel diffusion is given by "pore" defects, similarly to what was observed in lamellar phases.

Introduction

Thermotropic ionic liquid crystals (ILCs) are mesophases, *i.e.* liquid crystal (LC) phases, formed by ions. The most common cases reported in the literature are those where the salt is composed of a quaternized nitrogen cation, such as imidazolium, pyridinium, guanidinium, pyrrolidinium, and an inorganic anion, such as halides, PF_6^-, BF_4^-, $(CF_3SO_2)_2N^-$. These systems are often Ionic Liquids (ILs) but in cases where one or more alkyl chains are sufficiently long, microphase segregation occurs between the ionic moieties and the hydrophobic chains. Therefore smectic, that is layered, mesophases are observed, with an alternation of ionic and hydrophobic layers[1–15] with a few notable exceptions where a nematic phase has been reported.[14,16–18] Recent reviews highlight the state of the art in this field.[19–21]

Molecular dynamics (MD) simulations of ILCs are particularly demanding since these systems are usually very viscous due to the combination of long range electrostatic interactions, as in ILs, with the ordered structure typical of the liquid crystals. Not surprisingly, novel Coarse-Grained Force Fields (CGFFs) continue to appear in the literature both for the MD simulations of ILs[22,23] as well as for the MD simulations of LCs.[24–28] An easy prediction is therefore that CGFFs are going to play an important role in the description of the structural properties of thermotropic ILCs, as is already the case for the analogous class of compounds, surfactants and membranes.[29–33] An interesting review summarises the state of the art in coarse-graining techniques.[34]

In a recent paper we have reported the structural properties of the crystal B, smectic A and isotropic phases of the model ionic liquid crystal 1-hexadecyl-3-methylimidazolium nitrate obtained using MD simulations.[35] The force field used was a CGFF model recently developed for the isotropic phase of ionic liquids, that is short chain imidazolium salts.[36,37] The results of the simulation demonstrated that the CGFF exhibits mesomorphism; in particular, as found for the real salt, the bilayered ionic smectic A mesophase is observed, though in a range of temperatures higher than the experimental case; this might be expected, since, as thoroughly discussed in ref. 35 the reproduction of the transition temperatures of LC phases requires a very careful adjustment of the parameters of atomistic FFs.[38,39]

In a second paper, a detailed investigation of the dependence of the structural features of 1-alkyl-3-methylimidazolium salts as a function of the alkyl chain length, using the same CGFF, has been performed.[40] The results obtained confirmed that this CGFF model potential is capable of capturing the essential features that drive the formation of ionic mesophases.

Dynamical properties obtained from coarse-grained MD simulations suffer from an unphysical acceleration due to the smoothening of the potential energy surface introduced by the coarse-graining mapping. Indeed a more faithful representation of the dynamics using a CGFF has been obtained using a multiscale formalism.[41] Nevertheless, we still use here the original CG implementation as in ref. 35 for two reasons: first in this way we complete the characterization of the behaviour of the CGFF also from a dynamical point of view, after the structural characterization; and secondly we believe that the relative values of the dynamical properties or mechanisms of diffusion in

[a]*Istituto per la Tecnologia delle Membrane del CNR, Unità di Padova, and Department of Chemical Sciences of the University, Via Marzolo, 1-35131, Padova, Italy. E-mail: giacomo.saielli@unipd.it*

[b]*Department of Chemistry, James Franck Institute, and Computation Institute, University of Chicago, 5735 S. Ellis Ave., Chicago, Illinois, 60637, USA*

[c]*State Key Laboratory of Theoretical Physics, Institute of Theoretical Physics, Chinese Academy of Sciences, 55 East Zhongguancun Road, PO Box 2735, Beijing, 100190, China*

† Electronic supplementary information (ESI) available: Snapshots of the simulations discussed in the text. See DOI: 10.1039/c3sm50375e

anisotropic environments are still correct at a semi-quantitative level, thus providing a description of the dynamics of ionic smectic mesophases.

Diffusion in smectic A phases of thermotropic non-ionic LCs has been widely investigated by experiments,[42–46] theories[47–50] and computer simulations.[51–56] In all these works, special attention has been paid to the diffusion anisotropy, that is the ratio of the parallel, $D_{\|}$, *vs.* perpendicular, $D_{\perp}$, diffusion coefficient. The former accounts for the diffusion across the layers (parallel to the director) while the latter one for the diffusion in the plane of the layers (perpendicular to the director). The molecular motion parallel to the director is affected by a periodic potential that is expected to slow down the dynamics. In several cases, however, a nematic-like behaviour has also been observed in the smectic A phase, that is a behaviour where $D_{\|} > D_{\perp}$.[46,57] This behaviour has also been confirmed by MD simulations of model mesogens.[53,58] In other cases the opposite result ($D_{\|} < D_{\perp}$) has been found.[42] More generally, in the SmA phase, the activation energies of the parallel and perpendicular diffusions are different, therefore, if the phase is stable for a sufficiently large temperature range, an inversion of the $D_{\|}/D_{\perp}$ ratio can be observed as a function of the temperature, with the parallel diffusion coefficient being larger than the perpendicular one close to the smectic A–nematic (or –isotropic) transition and the opposite at lower temperatures.[43] A striking example of the dependence of the $D_{\|}/D_{\perp}$ ratio on the details of the molecular structure can be found in ref. 44 where the replacement of the cyano group by a trifluoromethoxy group in a 4-octyloxy-*N*-(4-X-benzylidene)aniline, X = CN, CF_3O, led to an inversion of the self-diffusion anisotropy. In any case, no matter which is the larger diffusion coefficient, the ratio has been often observed to be not too far from unity, usually between about 0.3 and 3.

A different situation is found, instead, for lamellar phases of surfactant–water mixtures. Here the layers are not only physically separated but also chemically distinct: a hydrophobic layer of the surfactant molecules, typically with a long alkyl chain, is followed and preceded by a water/ionic layer. The potential opposing the parallel diffusion is now expected to be much larger since it is requested that either a water molecule crosses a hydrophobic layer or that a hydrophobic molecule crosses a water layer. In fact, experimental data on several surfactant–water systems in the lamellar phase point to a large diffusion anisotropy, with the parallel diffusion coefficient smaller by a factor of about 25–30 or more than the perpendicular diffusion coefficient, both for the water and the surfactant molecules.[59]

Another important issue discussed in the literature is the mechanism of diffusion, especially that one parallel to the director. For thermotropic smectic A phases two different processes are conceivable: a direct "permeation" through the layer's boundary or a "parking-lot" mechanism where molecules first move in between the layers, orienting perpendicularly to the director, and then diffuse into the adjacent layer (or back into the original one).[60] The former mechanism has received larger credit, including the recent direct experimental observation in the smectic phase of filamentous bacteriophage fd.[61] The diffusion proceeds through "jumps" between adjacent layers, rather than following a Brownian motion. This also accounts for two, at first sight contradictory, facts: (i) existence of layers and (ii) the faster, or at least comparable, parallel diffusion compared to the perpendicular diffusion. The other mechanism has been suggested to become important for mixtures of hard rods and spheres, where the spheres arrange themselves at the boundary of the smectic phase thus facilitating the population of the interlayer region by rods oriented roughly perpendicularly to the director. This result obtained by Cinacchi and de Gaetani[58,62] is particularly interesting concerning ILCs that, apart from the presence of charges, are usually composed of stoichiometric mixtures of rod-like cations, though highly flexible, and more or less spherical anions.

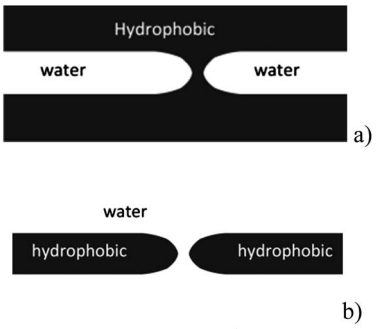

Fig. 1 Schematic representation of (a) neck and (b) pore defects in lamellar phases of surfactant–water mixtures.

In the case of lamellar phases of surfactant–water mixtures the slower parallel diffusion is thought to proceed mainly through defects in the structure. "Necks" and "pores" are the two primary point defects that can be formed in a lamellar phase. The former type connects two hydrophobic layers while the latter one connects two water layers, as in Fig. 1.

Constantin and Oswald[63] have investigated the diffusion in the lyotropic system $C_{12}EO_6$–H_2O using hydrophobic and hydrophilic probe molecules and found that the parallel diffusion coefficient for both probes is much smaller than the perpendicular one, by 10 to 40 times, depending on the temperature. However $D_{\|}$ of the hydrophobic probe increases exponentially close to the transition to the isotropic phase while $D_{\|}$ of the hydrophilic probe remains constant. This observation suggests that, in this system, neck-type defects develop on increasing the temperature.

Results and discussion

The model system and computational details

The basic ingredients of the CGFF model system have been described in ref. 36 and 37 while ref. 35 contains the details of the generation of the trajectory files used here for the analysis of the dynamical properties.

Briefly, the ion pair 1-hexadecyl-3-methylimidazolium nitrate is composed of 65 atoms. The CGFF reduces the number of particles to 19 by replacing each methyl and methylene unit, the imidazolium ring and the anion with single interaction sites, see Fig. 2. The figure shows the imidazolium ring (A); the methyl group on nitrogen 3 (B); the methylene group on

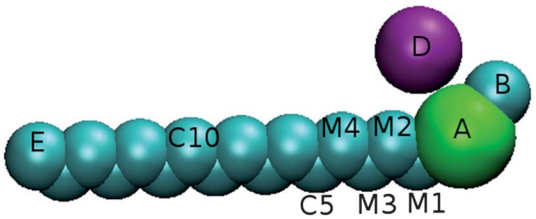

Fig. 2 Coarse-grained model of 1-hexadecyl-3-methylimidazolium nitrate with site labelling.[36,37]

nitrogen 1 (M1) and the next three methylene groups (M2, M3, M4) of the alkyl chain; the remaining 11 methylene groups of the chain (C); the methyl group C16 (E); and the anion (D).

Simulations have been run in the NPT ensemble with the software DL_POLY Classic.[64] Each trajectory file used for the analysis contains 1000 configurations saved every 27 ps.

Results

We briefly recall here the phase behaviour of the model system under investigation. A detailed description can be found in ref. 35. The model system exhibits three phases: a crystal B phase, up to *ca.* 500 K; a bilayered smectic A phase, between *ca.* 500 K and *ca.* 560 K; and an isotropic phase for temperatures higher than 560 K. A snapshot of the three structures can be found in Fig. 1 of ESI.†

We should mention that in the simulations we used orthorhombic periodic boundary conditions, where the ratio of the z box length and the x or y box length (box anisotropy) was fixed based on experimental layer thickness of the SmA phase.[35] Thus, these boundary conditions are fully compatible with the symmetry of the smectic and isotropic phases. Clearly we cannot reproduce here the triclinic structure of the low temperature crystal phase experimentally observed for long-chain imidazolium salts,[65] which is, however, beyond the scope of the present investigation. Thus the crystal B phase exhibited by the model system under orthorhombic periodic boundary conditions will serve as an interesting ordered phase for comparison with the smectic phase. A snapshot of the hexagonal arrangement in the CrB structure is shown in Fig. 2 of ESI.†

In Fig. 3 we show the mean square displacement functions, eqn (1), in the crystal B phase, for the A site (the cation head), the D site (the anion) and the E site (the cation tail) along the three box axes corresponding to the layer plane (x and y) and to the director (z). From eqn (1) the diffusion coefficients along the directions x, y and z can be calculated as the slope at long times of $\mathrm{MSD}_\alpha/2t$, where t is the time. Here we have consistently evaluated the diffusion coefficients by linear fitting in the range 2.5–15 ns. To estimate the errors in the values of the diffusion coefficients we have compared the two in-plane coefficients, D_x and D_y. They should be the same in all phases, since the director is along z in the crystal B and smectic A phase and for the isotropic phase there is no preferred direction. The discrepancy observed from the two fittings has been taken as an estimate of the error. Three temperatures have been selected corresponding

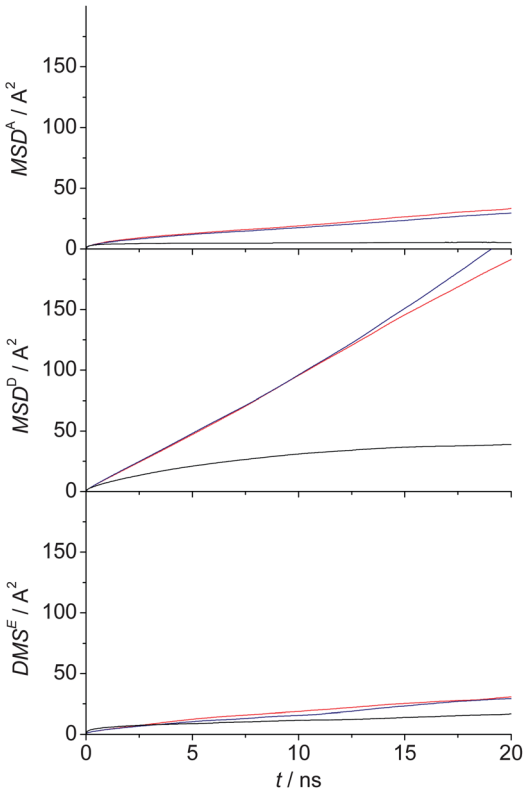

Fig. 3 Mean square displacements along the (red) x, (blue) y and (back) z coordinates of sites (top) A, (middle) D and (bottom) E for the crystal B phase at 450 K.

to the crystal B phase at $T = 450$ K, the smectic A phase at $T = 505$ K and the isotropic liquid phase at 600 K.

$$\mathrm{MSD}_\alpha = \langle |r_\alpha(t) - r_\alpha(0)|^2 \rangle,\ \alpha = x, y, z \qquad (1)$$

In Table 1 we report the values of the diffusion coefficients obtained as mentioned above.

In the crystal B phase neither the cation nor the anion can escape from the ionic layer, at least not during the 27 ns of the production run, since this would require crossing a well ordered hydrophobic region of alkyl chains arranged in a hexagonal fashion. Thus, the MSD of A and D sites along z at 450 K shows an upper limit. In contrast, the in-plane diffusion is not limited by a mean field potential and the MSD function has a clear linear behaviour. The anion diffusion coefficient D^{D}_{xy}(450 K) appears to be about eight times larger than the corresponding value of the cation site A. Cation tails, site E, have similar dynamics to the cation heads.

It is then instructive to analyse the mechanism of partial diffusion of cations along the z direction. In Fig. 4 we show the

Table 1 Diffusion coefficients (10^{-11} m^2 s^{-1}) in the three phases

T/K	D^{A}_z	D^{D}_z	D^{A}_{xy}	D^{D}_{xy}
450	0.0	0.0	0.6 ± 2	4.8 ± 2
505	12 ± 4	18 ± 4	24 ± 4	36 ± 4
600	66 ± 6	105 ± 6	75 ± 6	108 ± 6

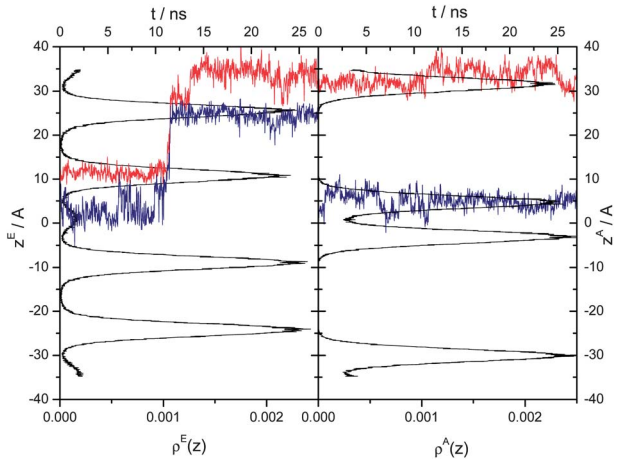

Fig. 4 Trajectory of the *z* coordinate of two molecules (in blue and red) in the crystal B phase at 450 K. (Left) Cation tail, site E; (right) cation head, site A. In black the density profile, $\rho(z)$, of (left) cation tail, site E; (right) cation head, site A.

trajectory of two molecules: the first one (blue) was, at time $t = 0$, fully laying in the ionic layer, thus essentially oriented in the *xy* plane, while the second one belonged to the top layer, oriented along the director. We stress here that the choice of the two molecules has been done after visual inspection of the trajectories, both for the CrB phase here and the SmA phase below; no particular meaning should be attributed to the selected molecules except that their detailed description will offer useful insights and an easier understanding of the diffusion mechanisms and their dependence on the phase structure and director orientation.

As we can see after about 11.3 ns the first molecule pushes the second one out of its layer into the ionic layer above and replaces it in the hexagonal packing of the chains. In Fig. 3 of ESI† we show the snapshots corresponding to this mechanism. It is clear, then, that a cation having the head in a given ionic layer is only allowed to displace its alkyl chain between the two adjacent layers without allowing the pivotal site A to change its position, except within the limited region of its ionic layer. Therefore any cation that changes its hydrophobic layer also inverts its orientation by 180°.

More interesting is the dynamics observed in the smectic A phase. As reported in ref. 35 the order, both orientational and translational, of the phase obtained from the model system is rather low compared to real non-ionic smectic phases made by rigid or only partly flexible molecules. The imidazolium cation is, instead, very flexible and lacks a real rigid anisotropic core. The orientational order parameter obtained from the simulations is, in fact, close to that one observed in phospholipid membranes.[35,66,67] Thus the smectic phase is formed essentially because of micro-segregation between ionic and hydrophobic regions; in contrast, an important mechanism in the stabilization of non-ionic smectic phases is the increased orientational order of the rigid core which enhances the translational order.[68] Moreover, in non-ionic smectic phases there is just one kind of molecules, therefore the layers of the rod-like particles are separated only by a more or less well defined boundary region. In contrast, in smectic ionic phases there is an alternation of layers (the hydrophobic one and the ionic one) both having a finite thickness and a different chemical composition. Here the thickness of the ionic layer is about 13.7 Å (the width at half height of $\rho^{A}(z) = \rho^{D}(z)$) while the width of the hydrophobic layer is 25.2 Å (as measured from the $\rho^{C5}(z)$ density profile, the first uncharged methylene group of the alkyl chain).[35] The two layers have rather blurred boundaries: it is possible to find alkyl chains in the ionic layer, as already observed for the crystal B phase, and also, at variance with the previous case, anions and cation heads in the hydrophobic layers.

The MSD functions in the smectic A phase at 505 K are shown in Fig. 5. Again the *x* and *y* components are almost overlapped and different from the *z* component, as expected for a uniaxial symmetry. The MSD functions are linear, except for the very beginning (up to *ca.* 2.5 ns). From the values in Table 1 we note that the anion diffusion coefficients, both the parallel and the in-plane component, are about 1.5 times larger than the corresponding values of the cation head, site A. For common ionic liquids based on short-chain quaternary nitrogen salts, in their isotropic phase, the anion is usually found to diffuse slightly slower or similarly to the cation.[69–74] Due to the strong electrostatic interactions, clusters, rather than single ions, exist in the liquid.[75–80] Thus the diffusion of cations and anions is not independent but strongly correlated so that both ions strongly affect the diffusion of their partner. However, in this case, because of the significantly different size and molecular weight of the cation and anion of $[C_{16}mim][NO_3]$, it is not surprising that the anions diffuse slightly faster than the cations. It is

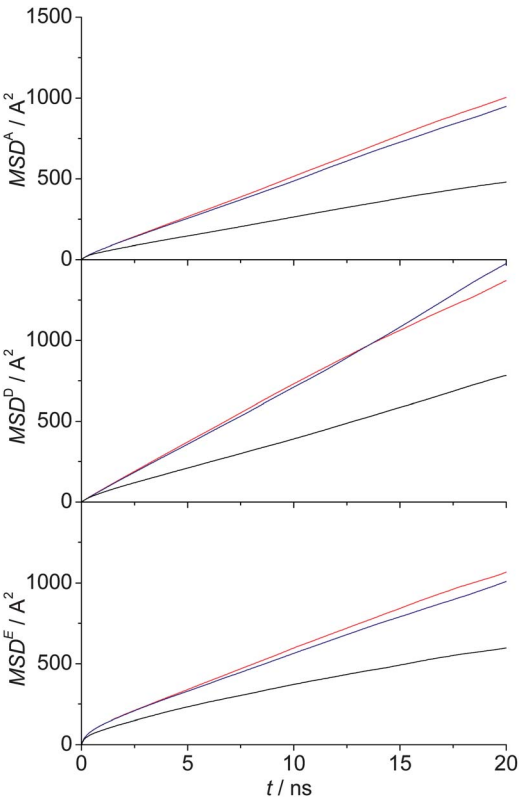

Fig. 5 Mean square displacements along the (red) *x* (blue) *y* and (back) *z* coordinates of sites (top) A, (middle) D and (bottom) E. Smectic A phase at 505 K.

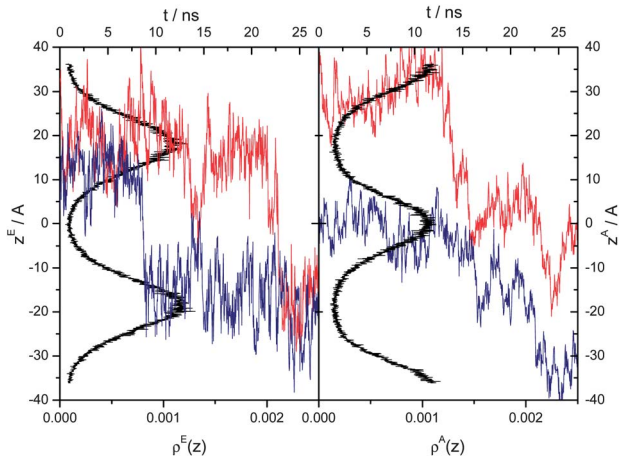

Fig. 6 Trajectory of the *z* coordinate of two molecules (in blue and red) in the smectic A phase at 505 K. (Left) Cation tail, site E; (right) cation head, site A. In black the density profile, $\rho(z)$, of (left) cation tail, site E; (right) cation head, site A.

noteworthy that in the smectic A phase, in contrast to the behaviour observed in the crystal B phase, the crossing of the hydrophobic layer by the charged species is allowed, as will be shown below.

Another relevant result is the relative value of the in-plane and parallel diffusion coefficients, for both cation and anion: the diffusion within the layers (*x* and *y* components) is twice as fast as the diffusion along the director (*z* component). This is expected, as mentioned already, because of the presence of a modulated mean field potential along the director. This result is in agreement with the behaviour observed in thermotropic non-ionic smectic LCs, having a self-diffusion anisotropy not far from unity while, as mentioned in the Introduction, the anisotropy in the lamellar phase of surfactant–water mixtures is much larger.

As far as the mechanism of diffusion is concerned we first highlight the behaviour of two molecules selected from the trajectory, see Fig. 6.

In contrast to what was found in the crystal B phase there is no concerted mechanism here, with one molecule replacing another one in the hexagonal lattice, since the chains in the hydrophobic layers are completely melted. As an example (snapshots can be found in Fig. 4 and 5 of ESI†), the first molecule (blue) in Fig. 6 is initially roughly aligned with its head in the middle ionic layer (see Fig. 6, right) and the tail in the top hydrophobic layer (Fig. 6, left). After about 8.5 ns the tail changes its position moving in the other hydrophobic layer while the head remains in the same ionic layer up to about 15 ns. The reorientation is similar to the only mechanism observed in the crystal B phase where the cationic head plays a pivotal role. However after about 15 ns the cation head begins to migrate through the hydrophobic layer rather smoothly with no apparent jumps reaching, at the end, the other ionic layer at the bottom of the box. Thus this molecule, during the 27 ns length of the simulation, crosses one layer and keeps its original orientation. The other trajectory selected (red) shows a different behaviour: it is initially roughly aligned with the tail in the top hydrophobic layer and the head in the top ionic layer. After about 14.5 ns the tail moves down into the ionic layer below, pulling the head in the same layer, but then recoiling inside the original hydrophobic layer. The entire process amounts to a complete head–tail reorientation within one layer. However, after about 23 ns the alkyl chain is shifted to the other hydrophobic layer while keeping the head in the same ionic region, thus again the head acts as a pivot for the cation reorientation of the alkyl chain.

Finally, in Fig. 7, we show the mean square displacements obtained along the *x*, *y* and *z* directions of the box axis for the isotropic case. As expected they appear almost superimposed, though a slight divergence is observed at long times. However diffusion coefficients agree within the error of the numerical estimation. The anion diffusion is about 1.5 times faster than the cation, exactly as observed in the SmA phase both for the parallel as well as for the perpendicular diffusion coefficients.

Despite the fact that we are using a CGFF, the results obtained for the diffusion coefficients in Table 1 are comparable with experimental data of similar compounds. For example, the diffusion coefficients of octylcyanobiphenyl (8CB) in the SmA phase at room temperature are of the order of 2 and 1×10^{-11} m^2 s^{-1} for $D_{\parallel}$ and $D_{\perp}$, respectively;[57] at higher temperatures (456 K) the diffusion coefficients in the smectic A phase of terephtal-bis-4-*n*-butylaniline (TBBA) were found to be 4.6 and 14×10^{-11} m^2 s^{-1} for $D_{\parallel}$ and $D_{\perp}$, respectively;[42] significantly lower values are reported for the diffusion of

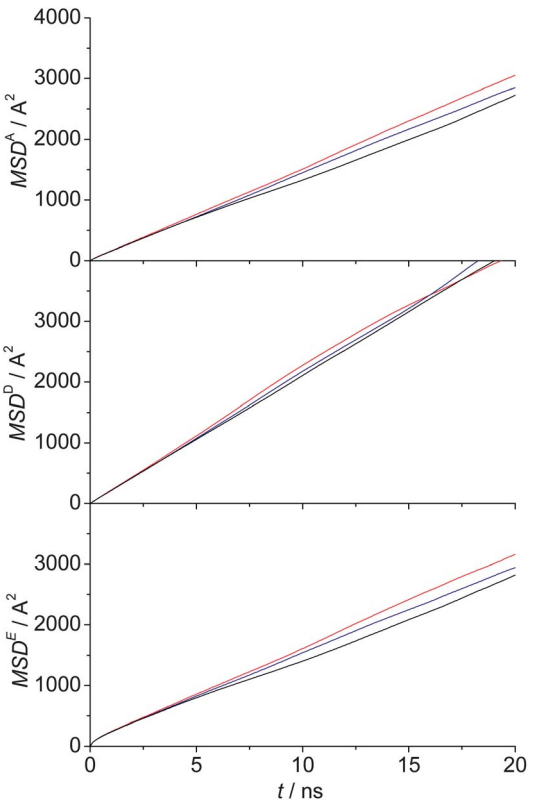

Fig. 7 Mean square displacements along the (red) *x* (blue) *y* and (back) *z* coordinates of sites (top) A, (middle) D and (bottom) E. Isotropic liquid phase at 600 K.

surfactant molecules in lamellar phases.[63,81] Therefore the model potential used here seems to give very reasonable results concerning the dynamical properties.

The examples discussed above for the diffusion in the SmA phase suggest that the pivot mechanism, the only one available in the crystal B phase (and that can only switch the position of a molecule between two adjacent hydrophobic layers having the ionic layer in common), is also operative and likely to occur in the smectic A phase, see the blue trajectory in Fig. 6; nevertheless also a direct permeation through the layers seems to occur, see the red trajectory in Fig. 6.

To have a more quantitative description of these processes in the SmA phase we can analyse more in detail the distribution of molecules aligned in a well defined direction (the z direction, that is along the director $\boldsymbol{n}$) at time zero, and how this distribution changes with time. However it is very difficult to analyse just the "orientation" of a cation since the molecule is highly flexible: a cation may have an "orientation" as defined by the orientation of the vector joining the imidazolium ring with the methyl carbon of the hexadecyl chain exactly aligned with the director but being significantly coiled as in Fig. 8(a). On the other hand, the arrangement of the chain as in Fig. 8(b), though the same vector is at an angle with the director $\boldsymbol{n}$, corresponds to a cation more aligned, as our intuition suggests, than in case (a). To overcome these difficulties in the evaluation of the cation orientation we proceed as follows.

The distance between the methyl carbon of the hexadecyl chain and the middle of the imidazolium ring in the all-trans arrangement is 20.9 Å (gas phase geometry optimized at the AM1 level). We select, from the history file, all the molecules that in the short initial time interval δt, between $t = 0$ and $t = \delta t$, have a projection on the z axis of the head-to-tail vector larger than half the full length of the molecule. This implies that the cations are at the same time mostly elongated and oriented along the director. For these molecules we evaluate the probability distribution of the above projection averaged over the time interval δt. Then we calculate the same probability (still averaged over a time interval of length δt) for the very same molecules that were initially selected, but now at later times, t_1, t_2, …, t_n. So, for example, the probability at t_j is the distribution of the projections of the orientational vector, as defined above, in the time interval between t_j and $t_j + \delta t$, for the same molecules that at the beginning had a projection larger than half the molecular length. In Fig. 9 we show the evolution of such probability distributions in the three phases for a choice of $\delta t =$ 270 ps and the times t_j of 0, 270 ps, 2.97 ns and 24.57 ns.

We discuss first the most obvious cases of the crystal B phase and the isotropic phase. In the crystal B phase (top panel of Fig. 9), according with the high order and viscosity of the system there is no appreciable variation of the distribution within the first *ca.* 25 ns of simulation. The distribution is strongly peaked (and it remains so) at a value corresponding to the length of the cation (the minus sign is due to the fact that we have focussed our attention on the molecules with a head-to-tail vector pointing downward). The opposite is true for the isotropic phase (bottom panel of Fig. 9). The initial distribution is, by definition, in the lower quarter of the allowed range. However, immediately in the second interval considered, from δt to $2\delta t$, it spreads up to the opposite border. The final distribution, already at equilibrium after less than 3 ns, is symmetrical and has a maximum at zero, that is for the head-to-tail vector laying in the plane, consistent with a completely random distribution of orientations and chain conformations.

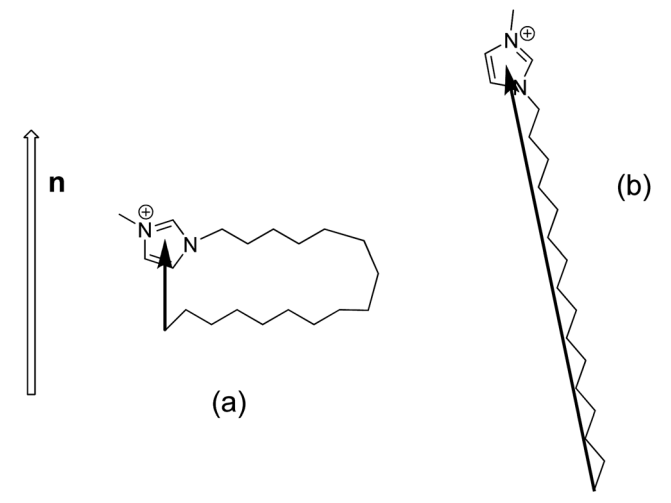

Fig. 8 Schematic representation of two possible orientations of the head-to-tail molecular vector.

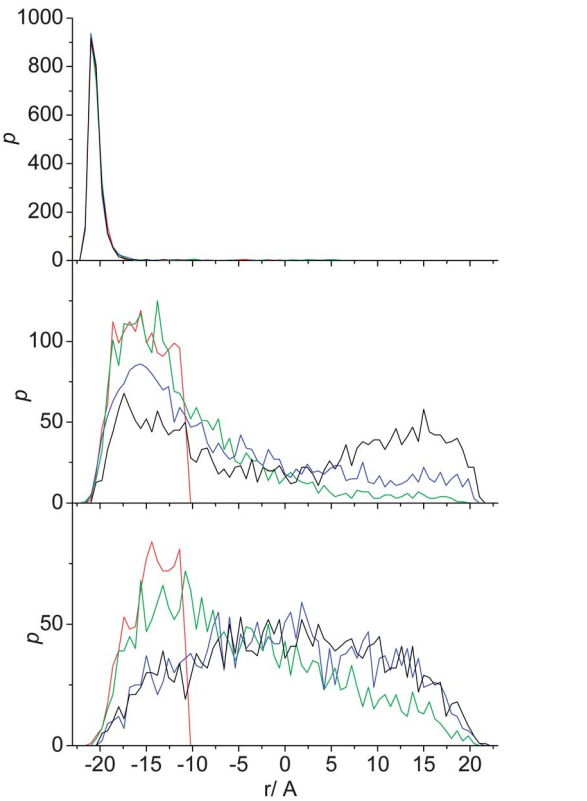

Fig. 9 Probability distribution p of the molecules having initially a z projection of the head-to-tail vector larger than half a molecular length (and here pointing to $-z$) at time (red) $t = 0$; (green) $t = 270$ ps; (blue) $t = 2.97$ ns; and (black) $t = 24.57$ ns.

In the SmA phase the profile of the distribution is more complex (middle panel of Fig. 9). The initial distribution is observed to spread towards the opposite range of values; however it does so by first increasing in the middle region where the projection of the head-to-tail vector is around zero. This corresponds to molecules that have lost their alignment and are now either strongly coiled, as in Fig. 8(a), or partly aligned perpendicularly to the director ***n***. Only at later times the probability increases markedly in the range between about 10 and 22 Å to assume, eventually, a bimodal distribution consistent with the presence of smectic layers of molecules each comprising two possible orientations. Such equilibrium distribution is reached with few tens of ns. It is interesting to note that the number of molecules, whose head-to-tail vector's projection is close to zero, is roughly constant during this process. This result supports the mechanism of diffusion coupled with a reorientation of the molecules.

However, a direct permeation is also possible: as mentioned in the Introduction, the presence of defects, either "necks" or "pores", connecting the hydrophobic and polar layers of a lyotropic lamellar phase may play an important role in the diffusion process. Therefore we have investigated whether the parallel diffusion of cations and anions occurs through a simple single molecule mechanism without a significant rearrangement of the local structure or if defects or restructuring of the environment do take place which favour and drive the layer crossing. To this end we have calculated the radial pair distribution function of sites A–D (the cation head and the anion), in the SmA phase at 505 K, separately for two sets of cations: (i) those cations whose site A is in the middle of the hydrophobic layer (presumably these are the molecules instantaneously involved in the diffusion across the layers, such as that one with the red trajectory in Fig. 6) and (ii) those cations whose site A is well within the ionic layer (presumably these are the molecules not involved, at that particular time, in a diffusion process along the director). Whether a cation belongs to one group or the other can be easily estimated from the density profile $\rho^{A}(z)$, see ref. 35. These two pair distribution functions, called hereafter *partial* $g^{AD}(r)$, are compared (lines in Fig. 10) with the analogous functions obtained without restrains on the molecule's position, the *total* $g^{AD}(r)$, in the isotropic phase and crystal B phase (symbols in Fig. 10) after the former two have been properly normalized so that they approach unity at long distances.

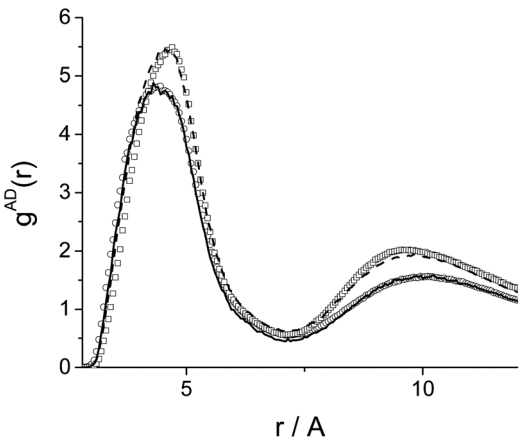

Fig. 10 Partial (lines) and total (symbols) pair correlation functions $g^{AD}(r)$. (Empty circles) Isotropic liquid at 600 K; (solid line) SmA phase at 505 K, for cations with the head in the hydrophobic layer. (Empty squares) CrB phase at 450 K; (dashed line) SmA phase at 505 K, for cations with the head in the ionic layer.

As we see in Fig. 10 the cation–anion correlation in the two phases, crystal B and isotropic liquid, as judged by the pair distribution function, is not strikingly different. A degree of similarity can be expected since the main process occurring, as the temperature is increased, is the melting of the alkyl chains, while the local arrangement of ions is known to be still relatively ordered, on a short length-scale, even in the isotropic phase of ionic liquids.[76,77] Nevertheless the *total* $g^{AD}(r)$ in the crystal B phase is more strongly peaked and has a maximum shifted lo larger separations (4.71 Å) compared to the *total* $g^{AD}(r)$ of the isotropic liquid phase (4.45 Å). Interestingly, the *partial* $g^{AD}(r)$ in the SmA phase for the molecules belonging to the hydrophobic layer is almost perfectly overlapped with the *total* $g^{AD}(r)$ of the isotropic liquid, while the *partial* $g^{AD}(r)$ in the SmA phase for the molecules belonging to the ionic layer is almost perfectly overlapped with the *total* $g^{AD}(r)$ of the crystal B phase. Small discrepancies can be attributed to the different temperatures. In other words, in the SmA phase those cations whose head resides in the ionic layer have a similar environment to the crystal B phase, while those cations whose head resides in the hydrophobic layer (the ones which are diffusing through the layers) have a similar environment to the isotropic liquid. This result, while confirming that the transition from the crystal B phase to the smectic A phase essentially amounts to a melting of the alkyl chains, also highlights the fact that the diffusion process of cations through the layers is accompanied by a local isotropization of the structure. Such defects, called pores in the terminology of lyotropic lamellar phases, which create channels for the communication between water layers (here, for this thermotropic smectic phase, the ionic layers) favour the crossing of the hydrophobic layers by the charged species. At the same time they are expected to slow down the in-plane diffusion of the alkyl chains since they interrupt the continuum hydrophobic layer.[81] In a different context, analogous "nematization", that is loss of translational order of the SmA phase during the parallel diffusion, was observed by computer simulations of mixtures of rods and spheres in ref. 58.

Conclusions

We have investigated the dynamical properties of a model CGFF of 1-hexadecyl-3-methylimidazolium nitrate. Despite the approximations intrinsic in the CGFF, the results obtained are in very reasonable agreement with the experimental data available for similar systems. We should mention, however, that a compensation of errors is likely to contribute to the good performance: while a CGFF has a faster dynamics compared to the corresponding atomistic FF,[82–84] it is well known that non-polarizable FFs for ionic liquids (such as that one from which our CGFF has been derived) suffer from a slower dynamics compared to experiments.[74,85] Nevertheless we believe that

relative values of parallel and perpendicular diffusion coefficients, as well as the mechanisms of diffusion, are qualitatively correct and offer a microscopic view of the dynamical processes occurring in the SmA phase of ILCs.

We have observed that both types of parallel diffusion mechanisms discussed in the literature concerning LCs take place: a "parking-lot" mechanism where the cation molecules first exit their hydrophobic layer, fluctuate inside the ionic layer and then can enter into the adjacent hydrophobic layer. This is not surprising since this mechanism, though unlikely in pure rod systems,[60,61] is strongly enhanced when rods are mixed with spheres.[58,62] It is noteworthy that the above reports are only concerned with non-ionic systems. An ILC is clearly not a simple mixture of rods and spheres but it does have indeed two components: the cation, rod-shaped, though highly flexible, and the anion, usually of a smaller and roughly spherical shape and, at variance with the rod–sphere mixtures mentioned above, there is a strong electrostatic attraction between unlike moieties and a strong electrostatic repulsion between like particles. Thus, the anions constitute a layer, together with the cation heads, in between the hydrophobic layers of the alkyl chains, exactly as the hard spheres microphase separate from the hard rods and arrange themselves in between the rod layers.[58,62]

On the other hand, we have observed the existence of defects in the layered structure, similar to what was reported for surfactant/water lamellar phases, which provide channels for diffusion through the layers by a local isotropisation of the structure. Such features are typical of charged species or strongly alternating polar/hydrophobic layers and are usually not observed in non-ionic mesophases.

These observations indicate that ILCs share structural and dynamical features with both non-ionic LC smectic phases and lamellar phases of surfactant–water mixtures, making them interesting new materials for applications in the field of solar cells,[86] membranes for water desalination,[87] battery materials[88] and electrochemical sensors.[89,90] In all these cases the microscopic arrangement of the ILC molecules and the conductive properties of the ionic mesophase have been found to have a significant impact on the performance of the ILC based devices compared, for example, to analogous devices based on isotropic ionic liquids. In turn this behaviour can only be rationalized and improved after we obtain a detailed understanding, at the molecular level, of their structure and dynamics and of the differences and similarities compared to the related compounds non-ionic LCs and lyotropic surfactants.

Acknowledgements

We thank Prof. A. Ferrarini (Università di Padova) and Dr G. Cinacchi (Universidad Autònoma de Madrid) for many valuable comments. Computer time was granted by CINECA (ISCRA project HP10BB7HYH) and the Laboratorio Interdipartimentale di Chimica Computazionale (LICC) of the University of Padova. Financial support from MIUR (PRIN HI-PHUTURE 2010N3T9M4_001, FIRB RBAP11C58Y_003 ''NanoSolar'') and Fondazione CARIPARO "Nano-Mode – Progetti di Eccellenza 2010" is also gratefully acknowledged. GS acknowledges the Royal Society of Chemistry for a JGA grant and the CNR-CAS bilateral agreement 2011–2013. YW thanks the financial support from the NSFC (nos 11274319 and 11121403) and the Hundred Talent Program of the CAS. GAV was supported by the Air Force Office of Scientific Research (AFOSR grant FA9550-10-1-0142).

Notes and references

1 W. Dobbs, L. Douce, L. Allouche, A. Louati, F. Malbosc and R. Welter, *New J. Chem.*, 2006, **30**, 528–532.
2 D. Pucci, G. Barberio, A. Bellusci, A. Crispini and M. Ghedini, *J. Organomet. Chem.*, 2006, **691**, 1138–1142.
3 F. Lo Celso, I. Pibiri, A. Triolo, R. Triolo, A. Pace, S. Buscemi and N. Vivona, *J. Mater. Chem.*, 2007, **17**, 1201–1208.
4 S. Sauer, S. Saliba, S. Tussetschlager, A. Baro, W. Frey, F. Giesselmann, S. Laschat and W. Kantlehner, *Liq. Cryst.*, 2009, **36**, 275–299.
5 V. Causin and G. Saielli, *J. Mater. Chem.*, 2009, **19**, 9153–9162.
6 X. Li, D. W. Bruce and J. M. Shreeve, *J. Mater. Chem.*, 2009, **19**, 8232–8238.
7 M. Blesic, M. Swadzba-Kwasny, J. D. Holbrey, J. N. Canongia Lopes, K. R. Seddon and L. P. N. Rebelo, *Phys. Chem. Chem. Phys.*, 2009, **11**, 4260–4268.
8 J. Carlos Diaz-Cuadros, L. Larios-Lopez, R. Julia Rodriguez-Gonzalez, B. Donnio, D. Guillon and D. Navarro-Rodriguez, *J. Mol. Liq.*, 2010, **157**, 133–141, DOI: 10.1016/j.molliq.2010.09.002.
9 T. Cardinaels, K. Lava, K. Goossens, S. V. Eliseeva and K. Binnemans, *Langmuir*, 2011, **27**, 2036–2043, DOI: 10.1021/la1047276.
10 K. M. Wiggins, R. L. Kerr, Z. Chen and C. W. Bielawski, *J. Mater. Chem.*, 2010, **20**, 5709–5714.
11 F. Xu, S. Matsubara, K. Matsumoto and R. Hagiwara, *J. Fluorine Chem.*, 2012, **135**, 344–349, DOI: 10.1016/j.jfluchem.2012.01.001.
12 Q. Zhang, K. Wang, Q. Ren, L. Niu and B. Chen, *Liq. Cryst.*, 2011, **38**, 1349–1355, DOI: 10.1080/02678292.2011.615946.
13 K. Tanabe, Y. Suzui, M. Hasegawa and T. Kato, *J. Am. Chem. Soc.*, 2012, **134**, 5652–5661, DOI: 10.1021/ja3001979.
14 B. Ringstrand, A. Jankowiak, L. E. Johnson, P. Kaszynski, D. Pociecha and E. Gorecka, *J. Mater. Chem.*, 2012, **22**, 4874–4880, DOI: 10.1039/c2jm15448j.
15 L. Casal-Dujat, O. Penon, C. Rodriguez-Abreu, C. Solans and L. Perez-Garcia, *New J. Chem.*, 2012, **36**, 558–561, DOI: 10.1039/c2nj20934a.
16 J. Baudoux, P. Judeinstein, D. Cahard and J. Plaquevent, *Tetrahedron Lett.*, 2005, **46**, 1137–1140.
17 K. Goossens, P. Nockemann, K. Driesen, B. Goderis, C. Goerller-Walrand, K. Van Hecke, L. Van Meervelt, E. Pouzet, K. Binnemans and T. Cardinaels, *Chem. Mater.*, 2008, **20**, 157–168.
18 W. Li, J. Zhang, B. Li, M. Zhang and L. Wu, *Chem. Commun.*, 2009, 5269–5271.
19 K. Binnemans, *Chem. Rev.*, 2005, **105**, 4148–4204.

20 K. V. Axenov and S. Laschat, *Materials*, 2011, **4**, 206–259, DOI: 10.3390/ma4010206.
21 V. Causin and G. Saielli, in *Green Solvents II. Properties and Applications of Ionic Liquids*, ed. A. Mohammad and D. Inamuddin, Springer, UK, 2012, pp. 79–118.
22 B. L. Bhargava, R. Devane, M. L. Klein and S. Balasubramanian, *Soft Matter*, 2007, **3**, 1395–1400.
23 C. Merlet, M. Salanne and B. Rotenberg, *J. Phys. Chem. C*, 2012, **116**, 7687–7693, DOI: 10.1021/jp3008877.
24 J. S. Lintuvuori and M. R. Wilson, *Phys. Chem. Chem. Phys.*, 2009, **11**, 2116–2125.
25 J. Zhang, J. Su, Y. Ma and H. Guo, *J. Phys. Chem. B*, 2012, **116**, 2075–2089, DOI: 10.1021/jp210764h.
26 B. Mukherjee, L. Delle Site, K. Kremer and C. Peter, *J. Phys. Chem. B*, 2012, **116**, 8474–8484, DOI: 10.1021/jp212300d.
27 M. Lamarra, L. Muccioli, S. Orlandi and C. Zannoni, *Phys. Chem. Chem. Phys.*, 2012, **14**, 5368–5375.
28 R. Pecheanu and N. M. Cann, *Phys. Rev. E: Stat., Nonlinear, Soft Matter Phys.*, 2010, **81**, 041704.
29 A. V. Sangwai and R. Sureshkumar, *Langmuir*, 2011, **27**, 6628–6638, DOI: 10.1021/la2006315.
30 R. J. Bingham and P. Ballone, *J. Phys. Chem. B*, 2012, **116**, 11205–11216, DOI: 10.1021/jp306126q.
31 D. Sergi, G. Scocchi and A. Ortona, *J. Chem. Phys.*, 2012, **137**, 094904–094910.
32 M. Huang, R. Kapral, A. S. Mikhailov and H. Chen, *J. Chem. Phys.*, 2012, **137**, 055101–055110.
33 M. A. Wilson and A. Pohorille, *J. Am. Chem. Soc.*, 1996, **118**, 6580–6587, DOI: 10.1021/ja9540381.
34 S. Riniker, J. R. Allison and W. F. van Gunsteren, *Phys. Chem. Chem. Phys.*, 2012, **14**, 12423–12430.
35 G. Saielli, *Soft Matter*, 2012, **8**, 10279–10287.
36 Y. Wang, S. Feng and G. A. Voth, *J. Chem. Theory Comput.*, 2009, **5**, 1091–1098, DOI: 10.1021/ct800548t.
37 Y. Wang, W. G. Noid, P. Liu and G. A. Voth, *Phys. Chem. Chem. Phys.*, 2009, **11**, 2002–2015, DOI: 10.1039/b819182d.
38 R. Berardi, L. Muccioli and C. Zannoni, *ChemPhysChem*, 2004, **5**, 104–111, DOI: 10.1002/cphc.200300908.
39 I. Cacelli, L. De Gaetani, G. Prampolini and A. Tani, *J. Phys. Chem. B*, 2007, **111**, 2130–2137, DOI: 10.1021/jp065806l.
40 Y. Ji, R. Shi, Y. Wang and G. Saielli, *J. Phys. Chem. B*, 2013, **117**, 1104–1109, DOI: 10.1021/jp310231f.
41 S. Izvekov and G. A. Voth, *J. Chem. Phys.*, 2006, **125**, 151101, DOI: 10.1063/1.2360580.
42 R. Blinc, M. Burgar, M. Luzar, J. Pirs, I. Zupancic and S. Zumer, *Phys. Rev. Lett.*, 1974, **33**, 1192–1195.
43 G. J. Krüger, H. Spiesecke, R. V. Steenwinkel and F. Noack, *Mol. Cryst. Liq. Cryst.*, 1977, **40**, 103–116, DOI: 10.1080/15421407708084474.
44 O. Oishi and S. Miyajima, *J. Magn. Reson.*, 2003, **160**, 74–77, DOI: 10.1016/S1090-7807(02)00110-6.
45 M. Cifelli, P. J. McDonald and C. A. Veracini, *Phys. Chem. Chem. Phys.*, 2004, **6**, 4701–4706.
46 S. V. Dvinskikh and I. Furo, *Phys. Rev. E: Stat., Nonlinear, Soft Matter Phys.*, 2012, **86**, 031704.
47 F. Volino and A. J. Dianoux, *Mol. Phys.*, 1978, **36**, 389–399, DOI: 10.1080/00268977800101641.
48 R. Tarroni and C. Zannoni, *J. Chem. Phys.*, 1991, **95**, 4550–4564, DOI: 10.1063/1.461833.
49 G. Moro and P. L. Nordio, *J. Phys. Chem.*, 1985, **89**, 997–1001, DOI: 10.1021/j100252a022.
50 A. Brognara, P. Pasini and C. Zannoni, *J. Chem. Phys.*, 2000, **112**, 4836–4848.
51 Y. Lansac, M. Glaser and N. Clark, *Phys. Rev. E: Stat., Nonlinear, Soft Matter Phys.*, 2001, **64**, 051703, DOI: 10.1103/PhysRevE.64.051703.
52 M. Cifelli, G. Cinacchi and L. De Gaetani, *J. Chem. Phys.*, 2006, **125**, 164912, DOI: 10.1063/1.2359428.
53 M. A. Bates and G. R. Luckhurst, *J. Chem. Phys.*, 2004, **120**, 394–403.
54 G. Cinacchi and L. De Gaetani, *Phys. Rev. E: Stat., Nonlinear, Soft Matter Phys.*, 2009, **79**, 011706.
55 A. Patti, D. El Masri, R. van Roij and M. Dijkstra, *J. Chem. Phys.*, 2010, **132**, 224907–224910.
56 A. Pizzirusso, M. Savini, L. Muccioli and C. Zannoni, *J. Mater. Chem.*, 2011, **21**, 125–133.
57 S. V. Dvinskikh, I. Furo, H. Zimmermann and A. Maliniak, *Phys. Rev. E: Stat., Nonlinear, Soft Matter Phys.*, 2002, **65**, 061701.
58 G. Cinacchi and L. De Gaetani, *J. Chem. Phys.*, 2009, **131**, 104908.
59 F. D. Blum, A. S. Padmanabhan and R. Mohebbi, *Langmuir*, 1985, **1**, 127–131, DOI: 10.1021/la00061a021.
60 J. S. van Duijneveldt and M. P. Allen, *Mol. Phys.*, 1997, **90**, 243–250, DOI: 10.1080/002689797172723.
61 M. P. Lettinga and E. Grelet, *Phys. Rev. Lett.*, 2007, **99**, 197802.
62 G. Cinacchi and L. De Gaetani, *Phys. Rev. Lett.*, 2009, **103**, 257801.
63 D. Constantin and P. Oswald, *Phys. Rev. Lett.*, 2000, **85**, 4297–4300.
64 W. Smith, T. R. Forester and I. T. Todorov, *DL_POLY Classic*, Daresbury Laboratory, UK, 2010.
65 C. K. Lee, H. W. Huang and I. J. B. Lin, *Chem. Commun.*, 2000, 1911–1912.
66 J. Douliez, A. Leonard and E. Dufourc, *Biophys. J.*, 1995, **68**, 1727–1739.
67 J. Douliez, A. Ferrarini and E. Dufourc, *J. Chem. Phys.*, 1998, **109**, 2513–2518, DOI: 10.1063/1.476823.
68 G. R. Luckhurst and G. Saielli, *J. Chem. Phys.*, 2000, **112**, 4342–4350, DOI: 10.1063/1.480981.
69 H. Tokuda, K. Hayamizu, K. Ishii, M. A. B. H. Susan and M. Watanabe, *J. Phys. Chem. B*, 2004, **108**, 16593–16600, DOI: 10.1021/jp047480r.
70 H. Tokuda, K. Hayamizu, K. Ishii, M. A. B. H. Susan and M. Watanabe, *J. Phys. Chem. B*, 2005, **109**, 6103–6110, DOI: 10.1021/jp044626d.
71 F. F. C. Bazito, Y. Kawano and R. M. Torresi, *Electrochim. Acta*, 2007, **52**, 6427–6437, DOI: 10.1016/j.electacta.2007.04.064.
72 M. B. Shiflett and A. Yokozeki, *J. Chem. Eng. Data*, 2007, **52**, 1302–1306, DOI: 10.1021/je700037z.
73 I. Nicotera, C. Oliviero, W. A. Henderson, G. B. Appetecchi and S. Passerini, *J. Phys. Chem. B*, 2005, **109**, 22814–22819, DOI: 10.1021/jp053799f.

74 A. Bagno, F. D'Amico and G. Saielli, *J. Mol. Liq.*, 2007, **131**, 17–23, DOI: 10.1016/j.molliq.2006.08.023.
75 J. Dupont, *Acc. Chem. Res.*, 2011, **44**, 1223–1231, DOI: 10.1021/ar2000937.
76 A. Bagno, F. D'Amico and G. Saielli, *ChemPhysChem*, 2007, **8**, 873–881, DOI: 10.1002/cphc.200600725.
77 A. Bagno, F. D'Amico and G. Saielli, *J. Phys. Chem. B*, 2006, **110**, 23004–23006, DOI: 10.1021/jp0659453.
78 Y. Wang and G. A. Voth, *J. Phys. Chem. B*, 2006, **110**, 18601–18608.
79 M. Gomes, J. Lopes and A. Padua, *Thermodynamics and Micro Heterogeneity of Ionic Liquids*, Springer, Berlin/Heidelberg, 2010.
80 J. N. A. Canongia Lopes and A. A. H. Pàdua, *J. Phys. Chem. B*, 2006, **110**, 3330–3335, DOI: 10.1021/jp056006y.
81 A. Yethiraj, D. Capitani, N. E. Burlinson and E. E. Burnell, *Langmuir*, 2005, **21**, 3311–3321, DOI: 10.1021/la046962r.
82 H. Qian, C. C. Liew and F. Muller-Plathe, *Phys. Chem. Chem. Phys.*, 2009, **11**, 1962–1969.
83 J. Wohlert and L. A. Berglund, *J. Chem. Theory Comput.*, 2011, **7**, 753–760, DOI: 10.1021/ct100489z.
84 S. J. Marrink, H. J. Risselada, S. Yefimov, D. P. Tieleman and A. H. de Vries, *J. Phys. Chem. B*, 2007, **111**, 7812–7824, DOI: 10.1021/jp071097f.
85 T. Yan, C. J. Burnham, M. G. Del Pòpolo and G. A. Voth, *J. Phys. Chem. B*, 2004, **108**, 11877–11881, DOI: 10.1021/jp047619y.
86 M. Yoshio, T. Ichikawa, H. Shimura, T. Kagata, A. Hamasaki, T. Mukai, H. Ohno and T. Kato, *Bull. Chem. Soc. Jpn.*, 2007, **80**, 1836–1841.
87 M. Henmi, K. Nakatsuji, T. Ichikawa, H. Tomioka, T. Sakamoto, M. Yoshio and T. Kato, *Adv. Mater.*, 2012, **24**, 2238–2241, DOI: 10.1002/adma.201200108.
88 M. Yoshio, T. Kagata, K. Hoshino, T. Mukai, H. Ohno and T. Kato, *J. Am. Chem. Soc.*, 2006, **128**, 5570–5577, DOI: 10.1021/ja0606935.
89 A. Safavi and M. Tohidi, *J. Phys. Chem. C*, 2010, **114**, 6132–6140, DOI: 10.1021/jp9114354.
90 N. V. Shvedene, O. A. Avramenko, V. E. Baulin, L. G. Tomilova and I. V. Pletnev, *Electroanalysis*, 2011, **23**, 1067–1072, DOI: 10.1002/elan.201000632.